MAGNETIC RESONANCE IMAGING OF PLAQUES IN A CYLINDRICAL CHANNEL

YUSUF, S. I.[1]*, AIYESIMI, Y. M.[1], JIYA, M.[1], AWOJOYOGBE, O. B.[2], & DADA, O. M.[2]
[1]Department of Mathematics and Statistics,
Federal University of Technology, Minna, Niger State, Nigeria
[2]Department of Physics,
Federal University of Technology, Minna, Niger State, Nigeria
***Email:** shakirudeen.yusuf@futminna.edu.ng **Phone No:** +234-706-929-7464

Abstract
The detection of blockage in cylindrical pipe using diffusion magnetic resonance equation has been carried out in previous works. In this study, Magnetic Resonance Imaging (MRI) is used to image the material causing the blockage of fluid in a cylindrical pipe. The Bloch Nuclear Magnetic Resonance (NMR) flow equation is solved analytically in cylindrical coordinates for flow of fluid in a radially symmetric cylindrical pipe. Based on the appropriate boundary conditions, the radial axis was varied to depict blockage in the pipe. The gradient pulse is designed such that it undergoes exponential rise and fall. The results show that the graphical pattern changed from vertical orientation (free flow) to horizontal orientation (partial blockage) – which is an indication of presence of materials that may cause obstruction to the fluid flow. Also, coagulation of colors indicates that obstruction caused is becoming more immense than previously noted. One similarity between the plaques imaged is that as the time is varied, they both show a drop in magnetization. This seems to lay credence to the fact that the model registers signal in its first few seconds or micro-seconds.

Keywords: Bloch NMR diffusion equation, Cylindrical pipe, Plaque

Introduction

Magnetic Resonance Imaging (MRI) is a recent approach adopted in the diagnosis of ailments and diseases in humans without surgical invasion. It can also be used to determine problems associated with blockage in cylindrical pipes. It provides accurate assessment of the individual component or multi-component systems in a matter of minutes whereas traditional radioactive tracer techniques may take weeks for each component (Awojoyogbe, *et al.,* 2011). This quick rate of assessment is possible because fluids exhibit random molecular motion of spins. This NMR spins are always in motion (Yusuf *et al.,* 2011). The rate of their signal loss or signal attenuation could be easily detected through magnetic resonance coupled with the fact that the molecules of fluids carry magnetic moments with them. This signifies whether or not a problem exists at any point in the flow field. Though not widely known, it has been noted for long that MRI is capable of quantifying diffusion movement of molecules because of uniqueness in relaxation times T_1 and T_2 (Yusuf *et al.* 2010).

There have been several methods adopted in detecting blockage in fluid pipeline. Yuan *et al.* (2014) used time splitting algorithms and Godunov mixed format to simulate the pulse propagation in the blocked pipelines. Another technique used by Sattar *et al.* (2008) is the system frequency response. This is a technique whereby the frequency response is used in the detection of partial blockages in a pipeline. Similar to this is the method adopted by Mohapatra *et al.*, (2006) for the detection of partial blockages in single pipelines by the frequency response method. Wang *et al.* (2005) also investigated analytically the effects of a partial blockage on pipeline transients. This is done when a partial blockage is simulated using an orifice equation. The influence of the blockage of flow in the unsteady pipe is then considered in the equation using a Dirac delta function.

Diffusion Magnetic Resonance Imaging (DMRI), being a viable alternative, is one of the most rapidly evolving techniques in the MRI field. Diffusion and flow can be measured very delicately and accurately using Magnetic Resonance Imaging (Hazlewood *et al.*, 1974). Coefficient of diffusion of a substance defined as the amount of material that diffuses in a certain time plays a vital role in the detection of blockage in a pipe using MRI. Random diffusion motion of water molecules has intriguing properties depending on the physiological and anatomical environment of the organisms being studied. These are the principles being exploited by the method of DMRI.

It is these same principles that we have applied to radially symmetric cylindrical pipe under the influence of radiofrequency field as a probe to perturb the molecules.

Material and Method

Following Yusuf *et al,* (2015), the diffusion magnetic resonance equation in a radially symmetric cylindrical coordinates is

$$\frac{\partial M_y}{\partial t} = D\left(\frac{\partial^2 M_y}{\partial r^2} + \frac{1}{r}\frac{\partial M_y}{\partial r} + \frac{\partial^2 M_y}{\partial z^2}\right) + \frac{F_o}{T_o}\gamma B_1(t) \quad (1)$$

and using the appropriate boundary conditions, we obtain the solution

$$M_y\,(r,z,t) = \frac{4\sigma_0}{\pi}\sum_{k=1}^{\infty}\sum_{m=1}^{\infty}\left\{\frac{(1-\cos k\pi)}{k\frac{s_m}{a}J_1(\frac{s_m}{a})}e^{-Dt(\frac{s_m}{a})^2+(\frac{k\pi}{L})^2}\right\}\left\{J_0\left(\frac{s_m}{a}r\right)\right\}\sin\frac{k\pi z}{L} + \frac{bF_o}{wT_o}\gamma\sin(wt) \quad (2)$$

where the diffusion coefficient $D = -\frac{V^2}{T_o}$ was accurately defined in terms of MRI flow parameters fluid velocity, v , T_1 and T_2 relaxation rates (as $T_0 = \frac{1}{T_1} + \frac{1}{T_2}$), $s_m = \gamma G\delta$ and $F_0 = \frac{M_0}{T_1}$, = gyromagnetic ratio, G = RF gradient pulse magnitude and = gradient pulse duration.

From equation (2), the transverse magnetization is given as follows:

$$M_y(r,z,t) = \frac{4\sigma_0}{\pi}\sum_{k=1}^{\infty}\sum_{m=1}^{\infty}\left\{\frac{(1-\cos k\pi)}{\mathrm{k}\pi\frac{s_m}{a}J_1\left(\frac{s_m}{a}\right)}\exp\left(-Dt\left(\frac{s_m}{a}\right)^2+\left(\frac{k\pi}{L}\right)^2\right)\right\}\left\{J_0\left(\frac{s_m}{a}r\right)\sin\left(\frac{k\pi z}{L}\right)\right\} + \frac{F_0}{T_0}\int_\delta^t \gamma B_1(t)dt \quad (3)$$

If the radio frequency (RF) magnetic field is defined as follows:

$$B_1(t) = G(t)r \quad (4)$$

Therefore, the integral becomes:

$$\frac{F_0}{T_0}\int_\delta^t \gamma B_1(t)dt = \frac{T_2 M_0 r}{T_1 + T_2}\int_\delta^t G(t)dt \quad (5)$$

If it is assumed that the gradient pulse $G(t)$**,** is designed such that $G(t)$ undergoes exponential rise and fall (Price, 1997, 1998 and Dada *et al.,* 2015), then we have:

$$G(t) = g\exp\left(-\frac{t}{T_1 + T_2}\right) \quad (6)$$

where g is the magnitude of the gradient pulse δ is the gradient pulse duration. The integral in equation (5) becomes:

$$\frac{F_0}{T_0}\int_{\delta}^{t}\gamma B_1(t)dt = -\frac{T_2 M_0 r}{T_1+T_2}(T_1+T_2)g\exp\left(-\frac{(t-\delta)}{T_1+T_2}\right) = -gT_2M_0 r\exp\left(-\frac{(t-\delta)}{T_1+T_2}\right) \quad (7)$$

Using equation (7) and setting $k = 1$, equation (3) becomes:

$$M_y(r,z,t) = \frac{4\sigma_0}{\pi}\sum_{m=1}^{\infty}\left\{\frac{(1-\cos\pi)}{\frac{s_m}{a}J_1\left(\frac{s_m}{a}\right)}\exp\left(-Dt\left(\frac{s_m}{a}\right)^2+\left(\frac{\pi}{L}\right)^2\right)\right\}\left\{J_0\left(\frac{s_m}{a}r\right)\sin\left(\frac{\pi z}{L}\right)\right\} - gT_2M_0 r\exp\left(-\frac{(t-\delta)}{T_1+T_2}\right) \quad (8)$$

$$M_y(r,z,t) = \frac{8\sigma_0}{\pi}\sum_{m=1}^{\infty}\left\{\frac{1}{\frac{s_m}{a}J_1\left(\frac{s_m}{a}\right)}\exp\left(-Dt\left(\frac{s_m}{a}\right)^2+\left(\frac{\pi}{L}\right)^2\right)\right\}\left\{J_0\left(\frac{s_m}{a}r\right)\sin\left(\frac{\pi z}{L}\right)\right\} - gT_2M_0 r\exp\left(-\frac{(t-\delta)}{T_1+T_2}\right) \quad (9)$$

For simulation, we consider oil wax and oil based mud as two plagues in the pipe. Given that $T_1 and\ T_2$ are the relaxation times of the fluid conditions within the pipe, as shown in table 1:

Table 1: Fluid Properties of Oil, Crude oil and Oil Wax

Materials	$\boldsymbol{T_1(s)}$	$\boldsymbol{T_2(s)}$	$\boldsymbol{D(cm^2s^{-1})}$	$\boldsymbol{D(m^2s^{-1})}$
Oil	0.84	0.325	0.0000052	5.2E-10
Crude Oil	0.5	0.486	0.000002	2.0E-10
Oil Wax	1.1195	0.5432	0.0000035	3.5E-10

NMR fluid properties at reservoir conditions are: B_o = 0.0176T, $TE = 1.2\,ms$, $G = 0.18\,G/cm$ (Coates *et al.*, 1999) where B_o is the static field; G is the gradient field and TE is the echo time.

As noted in earlier sections,

$$s_m = \frac{T_1}{T_2}\gamma g\delta(FOV) \quad (10)$$

where FOV is the field of view, g is the gradient pulse magnitude and δ is the gradient pulse duration. This expression indicates that the selection of a value for the index m is tantamount to the choice of an observed set of relaxation times. Since σ_o is a constant, it can be assumed that $\sigma_o = M_o$, Equation (9) for just a given set of relaxation times becomes:

$$M_y(r,z,t)|_{r_1 r_2} = \frac{8M_o}{\pi}\{\frac{1}{\left(\frac{T_1}{aT_2}\gamma g\delta(FOV)\right)J_1\left(\frac{T_1}{aT_2}\gamma g\delta(FOV)\right)}\exp[-Dt(\frac{T_1}{aT_2}\gamma g\delta(FOV))^2 + \left(\frac{\pi}{L}\right)^2\Big]\left\{J_o\left(\frac{T_1}{aT_2}\gamma g\delta(FOV)r\right]\sin\left(\frac{\pi z}{L}\right)\right\} - gT_2M_o r\exp\left(-\frac{(t-\delta)}{T_1+T_2}\right) \quad (11)$$

Results and Discussion

3.1 Imaging of Flow of Oil with Lateral Adjustments

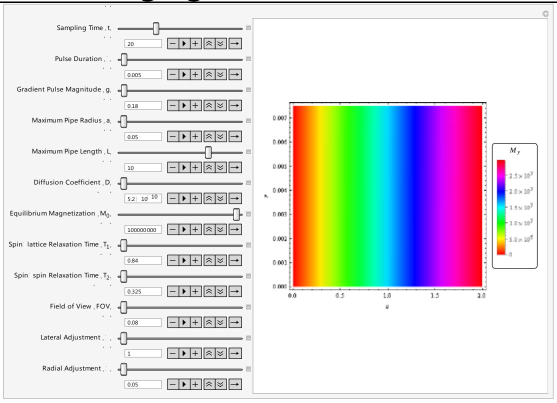

Figure 1a: Imaging of blockage with lateral adjustment = 1 and radial adjustment = 0.05

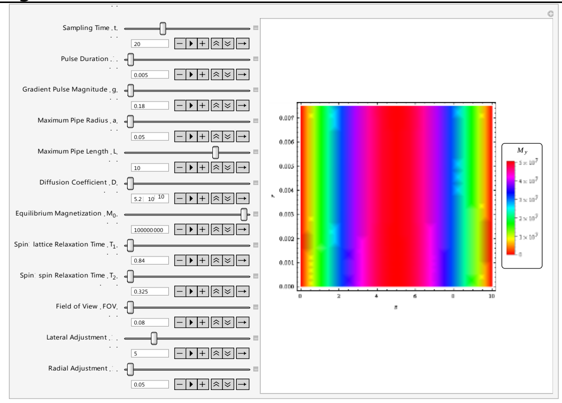

Figure 1b: Imaging of blockage with lateral adjustment = 5 and radial adjustment = 0.05

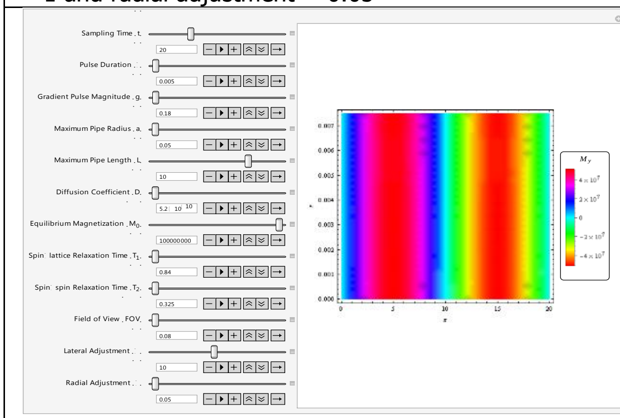

Figure 1c: Imaging of blockage with lateral adjustment = 10 and radial adjustment = 0.05

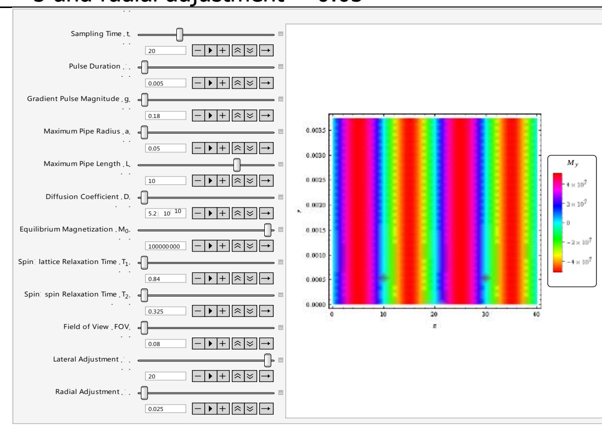

Figure 1d: Imaging of blockage with lateral adjustment = 20 and radial adjustment = 0.025

3.2 Imaging of Flow of Oil with Radial Adjustment

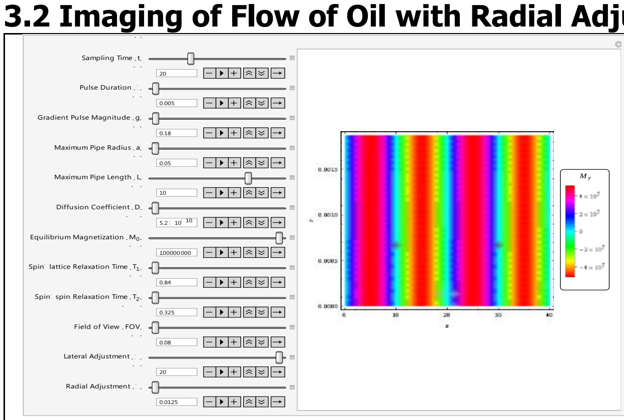

Figure 2a: Imaging of blockage with lateral adjustment = 20 and radial adjustment = 0.0125

3.3 Imaging of Flow of Oil with Time Adjustment

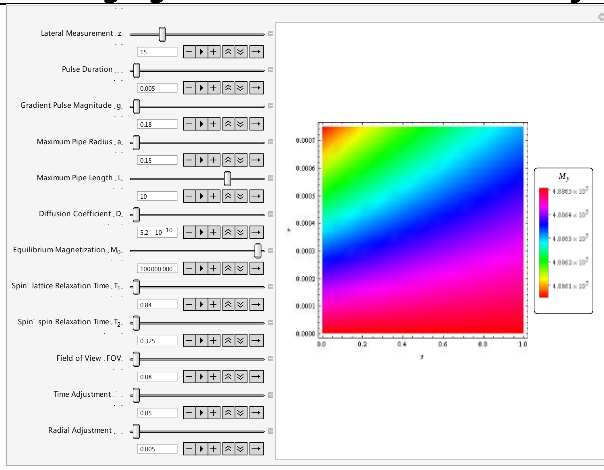

Figure 3a: Imaging of blockage with time adjustment = 0.05 and radial adjustment = 0.05

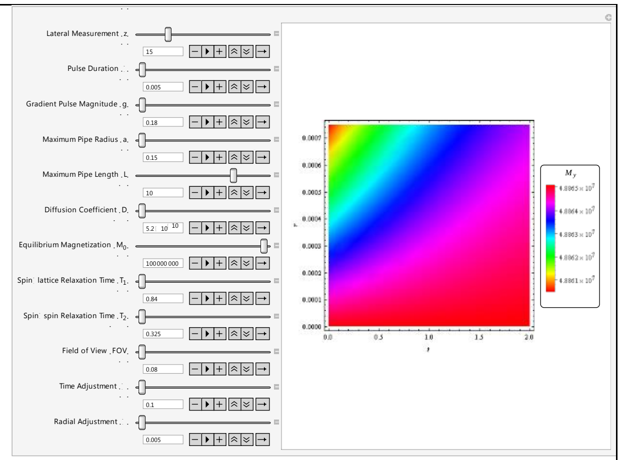

Figure 3b: Imaging of blockage with time adjustment = 0.1 and radial adjustment = 0.05

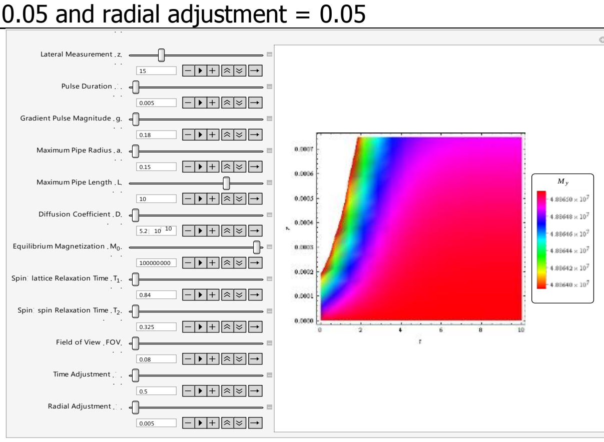

Figure 3c: Imaging of blockage with time adjustment = 0.5 and radial adjustment = 0.05

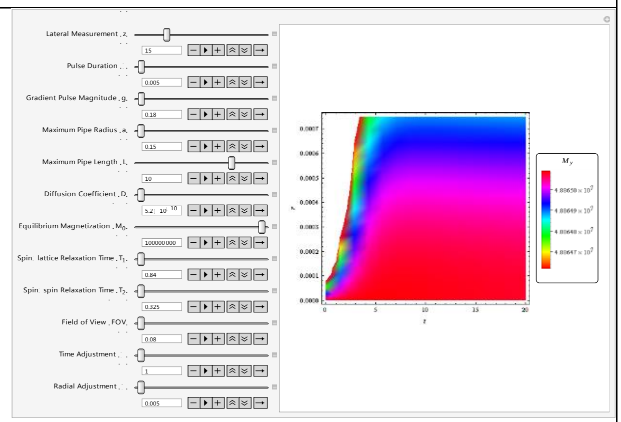

Figure 3d: Imaging of blockage with time adjustment = 1 and radial adjustment = 0.05

3.4 Imaging of Oil Wax as a Causative Agent of Blockage with Time Adjustment

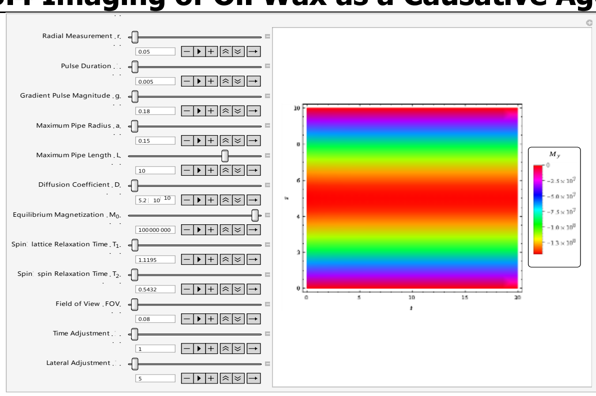

Figure 4a: Imaging of blockage with time adjustment =5 and radial adjustment = 0.005 for oil wax

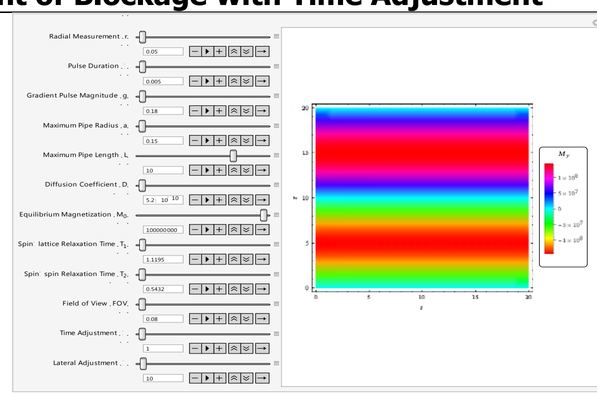

Figure 4b: Imaging of blockage with time adjustment =10 and radial adjustment =0.005 for oil wax

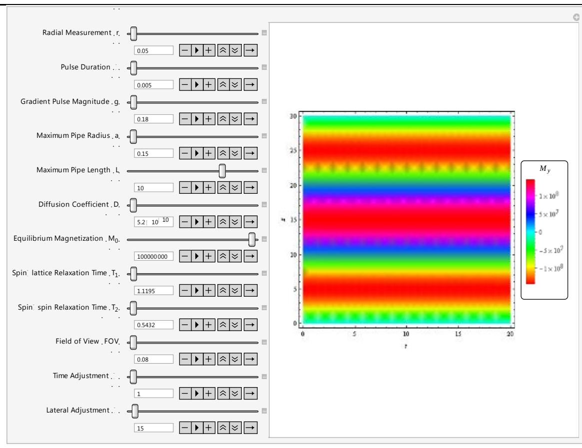

Figure 4c: Imaging of blockage with time adjustment = 15 and radial adjustment = 0.005 for oil wax

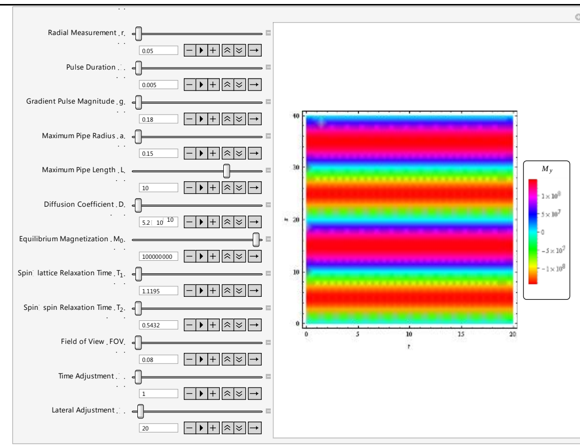

Figure 4d: Imaging of blockage with time adjustment = 20 and radial adjustment = 0.005 for oil wax

3.5 Imaging of Oil Based Mud (OBM) as a Causative Agent of Blockage with Time Adjustment

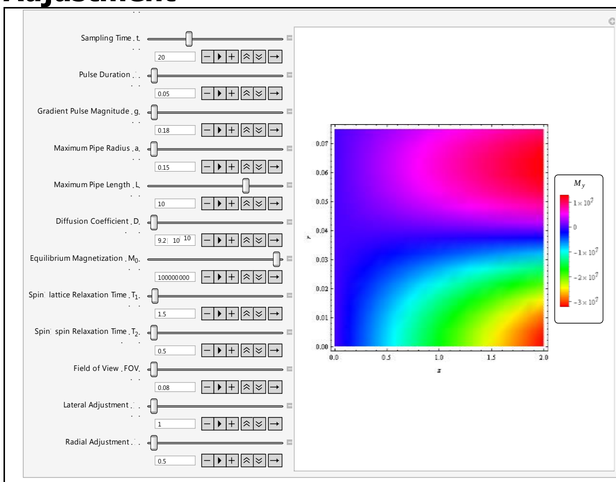

Figure 5a: Imaging of blockage with lateral adjustment = 1 and radial adjustment = 0.5 for mud

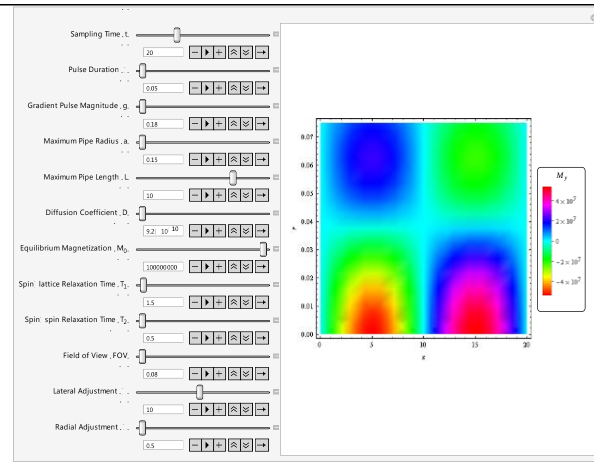

Figure 5b: Imaging of blockage with lateral adjustment =10 and radial adjustment = 0.5 for mud

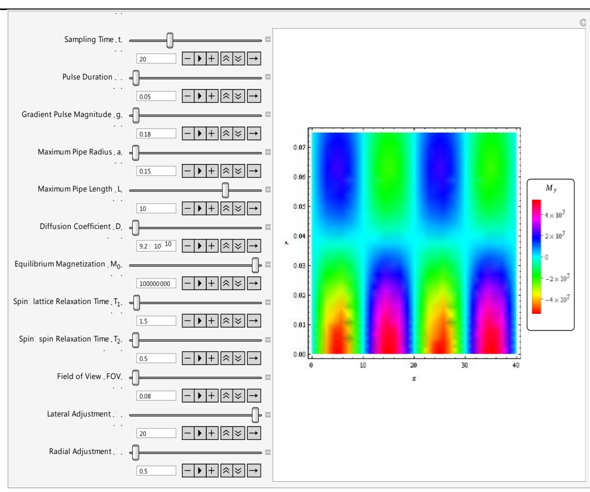

Figure 5c: Imaging of blockage with lateral adjustment = 20 and radial adjustment = 0.5 for mud

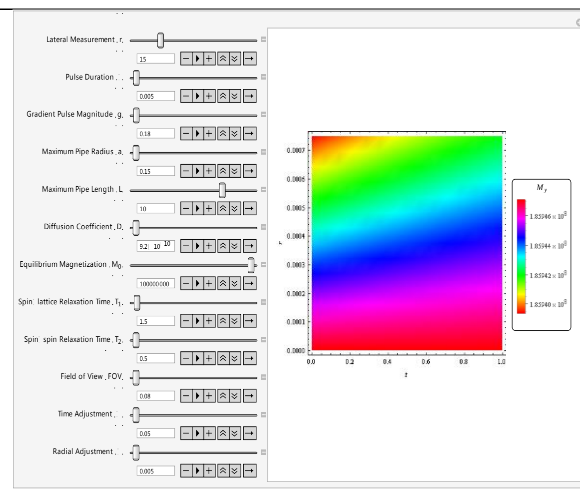

Figure 5d: Imaging of blockage with time adjustment = 0.05 and radial adjustment = 0.005 for mud

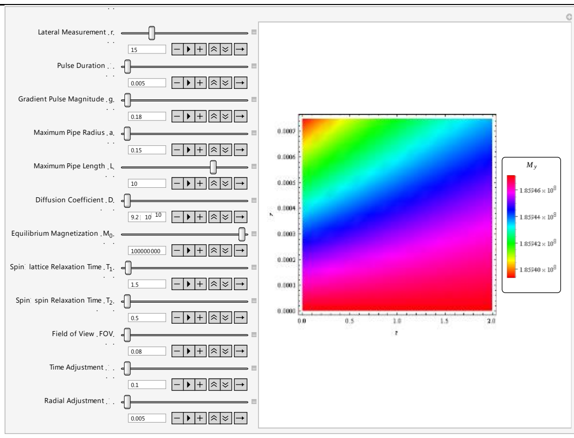

Figure 5e: Imaging of blockage with time adjustment = 0.1 and radial adjustment = 0.005 for mud

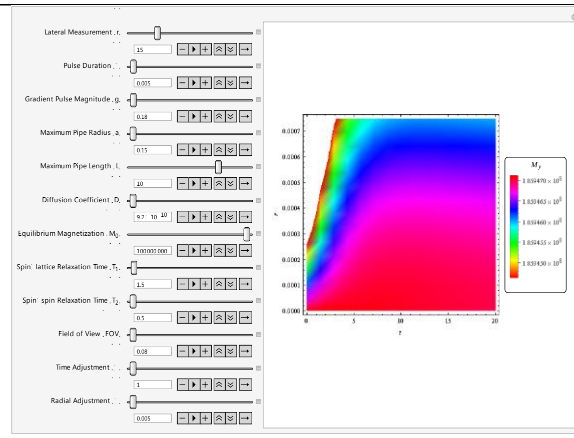

Figure 5f: Imaging of blockage with time adjustment =1 and radial adjustment = 0.005 for mud

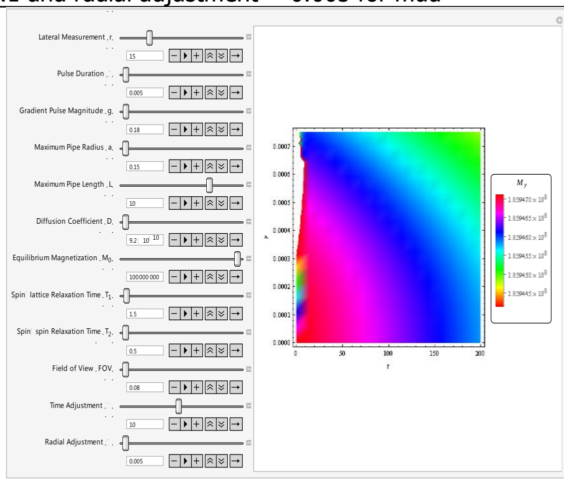

Figure 5g: Imaging of blockage with time adjustment =10 and radial adjustment =0.005 for mud

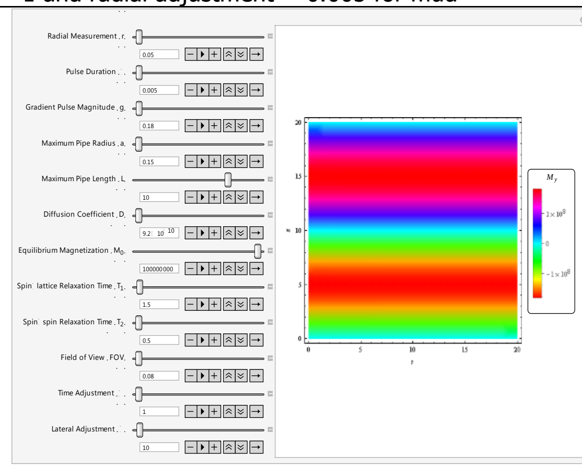

Figure 5h: Imaging of blockage with time adjustment =1 and lateral adjustment =10 for mud

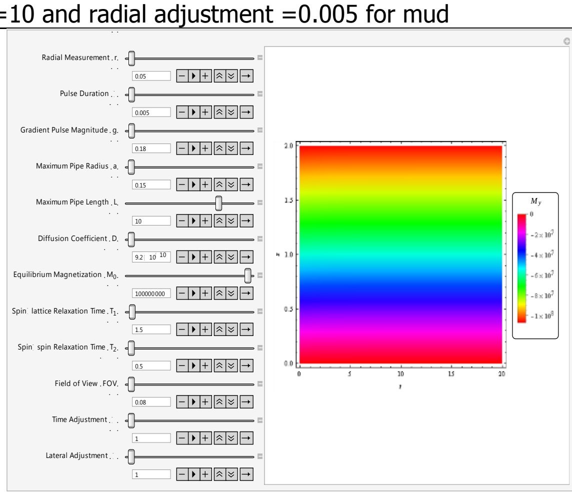

Figure 5i: Imaging of blockage with time adjustment =1 and lateral adjustment =1 for mud

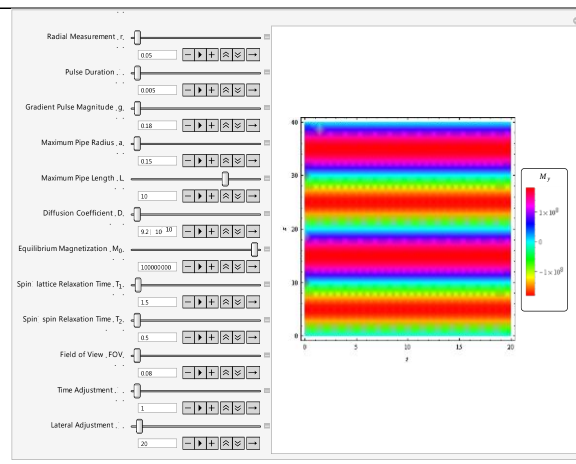

Figure 5j: Imaging of blockage with time adjustment =1 and lateral adjustment = 20 for mud

From equation (9) and using the relaxation parameters in Table 1, the possibility of performing computational MRI to image different components of obstruction or blockage in cylindrical pipe has been demonstrated. Unique images for oil, crude oil and wax were obtained. It would be observed that the images from oil are quite similar when values were varied laterally and radially

(Figure 1a-d and 2a). They have vertical orientation- an indication of free flow condition of the fluid.

However, from Figures 3a – d and 4a - d, the pattern changed from vertical to horizontal orientation with oil wax recording an initial negative magnetization. This is an indication of presence of materials that may cause obstruction to the fluid. More conspicuous is the pattern demonstrated by plots from the oil-based mud (figures 5a-5j). This coagulation of colors indicates that obstruction caused by mud can be more immense than that from oil wax.

Conclusion

Magnetic Resonance Imaging (MRI) has been used to image the materials causing the blockage of fluid in a cylindrical pipe. The gradient pulse is designed such that it undergoes exponential rise and fall. One similarity between the two plaques imaged is that as the time is varied, they both show a drop in magnetization. This seems to lay credence to the fact that the model registers signal in its first few seconds or micro-seconds. What is interesting in this work is that few NMR data are required for plaque imaging and the computational model is capable of interpolating for data points which are impossible to image directly because of NMR hardware restrictions.

Acknowledgment

Management of the Federal University of Technology, Minna is hereby acknowledged for sponsoring this research work.

References

Awojoyogbe, O. B., Faromika, O. P., Dada, M., & Dada, O. E. (2011). Mathematical concepts of the bloch flow equations for general magnetic resonance imaging. *A Review Part A*, 38A (3), 85-101.

Coates, G. R., Xiao, L. & Prammer, G. M. (1999). NMR logging principles and applications. Houston, USA: *Halliburton Energy Services.*

Dada, O. M., Awojoyogbe, O. B., & Ukoha, A. C. (2015). A computational analysis for quantitative evaluation of petrol-physical properties of rock fluids based on bloch NMR diffusion model for porous media. *Journal of Petroleum Science and Engineering*, 127, 137 – 147.

Hazlewood, C. F., Chang, D. C., & Nichols, B. L. (1974). Nuclear magnetic resonance relaxation times of water protons in skeletal muscle, *Journal of Biological Physics,* 14, 583-606.

Mohapatra, P., Chaudhry, M., Kassem, A., & Moloo, J. (2006). Detection of partial blockage in single pipelines. *Journal of Hydraulic Engineering*, 132(2), 200–206.

Price, W. S. (1997). Pulsed field gradient nuclear magnetic resonance as a tool for studying translational diffusion: Part I. Basic Theory. *Concepts of Magnetic Resonance*, 9, 299-336.

Price, W. S. (1998). Pulsed-field gradient nuclear magnetic resonance as a tool for studying translational diffusion: Part II. experimental aspects. *Concepts of Magnetic Resonance*, 10(4), 197-237.

Sattar, A., Chaudhry, M., & Kassem, A. (2008). Partial blockage detection in pipelines by frequency response method. *Journal of. Hydraulic Engineering*, 134(1), 76–89.

Wang, X., Lambert, M., & Simpson, A. (2005). Detection and location of a partial blockage in a pipeline using damping of fluid transients. *Journal of Water Resources, Planning and Management*, 131(3), 244–249.

Yuan, T., Xuefen, Z., Dan, T., Rui, W., & Huan, T. (2014). Applied mechanics and materials. *TransTech Publications, Switzerland Doi:10.4028/www.scientific.net/AMM.490-491.490*.

Yusuf, S. I., Aiyesimi Y. M., & Awojoyogbe, O. B. (2010). An analytic investigation of bloch nuclear magnetic resonance flow equation for the analysis of general fluid flow, *Nigerian Journal of Mathematics and Applications,* 20, 82 – 92.

Yusuf, S. I., Aiyesimi, Y. M., & Awojoyogbe, O. B. (2011). Effect of transverse relaxation rates on time-dependent magnetic resonance imaging, *African Journal of Physical Sciences,* 4(1), 119 – 126.

Yusuf, S. I., Aiyesimi, Y. M., Jiya, M., & Awojoyogbe, O. B. (2015). Detection of blockage in a radially symmetric cylindrical pipe using diffusion magnetic resonance equation. *Journal of Science, Technology, Mathematics and Education,* 11(3), 192 – 200.